ACS OMEGA

http://pubs.acs.org/journal/acsodf

Article

Hydrothermal Extraction of Amorphous Silica from Locally Available Slate

Usman Ghani, Shah Hussain, Asad Ali,* Vineet Tirth, Ali Algahtani, Abid Zaman,* Muhammad Mushtaq, Khaled Althubeiti, and Mohammed Aljohani

Cite This: *ACS Omega* 2022, 7, 6113−6120

Read Online

ACCESS | Metrics & More | Article Recommendations

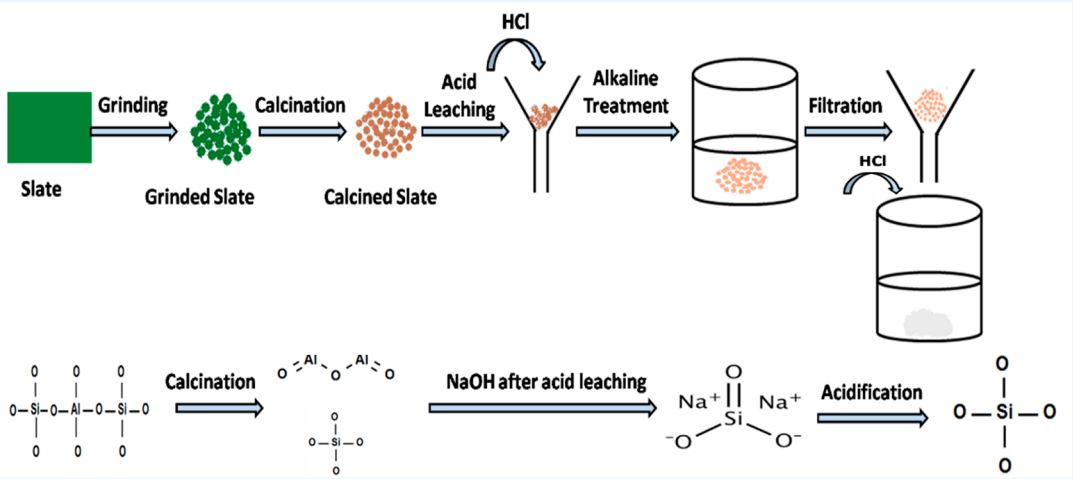

ABSTRACT: Slate is a naturally available aluminous silicate based material and can be used as a good source for silica extraction. In the current investigation, the slate sample was passed through calcination and acid leaching processes to decrease alumina contents and other major constituents. Silica extraction was performed by alkaline hydrothermal treatment of a given slate sample followed by acidic precipitation. Different steps, including the effect of concentration of sodium hydroxide solution, reaction time, the ratio of the mass of sample to volume of alkaline solution, the temperature of dispersion, and pH of the filtrate, were investigated to extract the maximum amount of pure amorphous silica. The extracted silica was physicochemically analyzed through XRF, XRD, FT-IR spectroscopy, and SEM techniques. The amorphous nature of the extracted silica is evident from XRD and SEM studies, while FT-IR studies support its purity, showing peaks of only Si−O−Si bonds. The purity of the extracted silica was further confirmed via XRF spectroscopic analysis and a hydrofluoric acid test.

INTRODUCTION

Silica (SiO_2) is an important constituent of many industrial products, including ceramics, electronics, and different polymeric materials. Because of its small particle size, silica has a wide range of applications in the fields of thermal insulation,[1] composite filler, catalysis, chromatography,[2] biological imaging, drug delivery systems, sensors, liquid armors, etc. In 1968, a first method was reported for obtaining monodispersed and spherical silica from tetraethyl orthodox silicate in basic medium by hydrolysis.[3] Because of the costly production of silica from tetraethyl orthodox silicate, other low-cost materials to extract silica at low cost have also been reported.[4] Sodium silicate solution has been used as an alternative for tetraethyl orthosilicate to extract silica at a low cost.[5] Sodium silicate solution was obtained by treating silica-rich waste materials, including rice husk ash, rice hull ash, bagasse bottom ash, semiburned rice straw ash, etc., with an alkali.[6,7] Silica was then precipitated from sodium silicate solution by acidification with an aqueous solution of hydrochloric acid or carbon dioxide gas,[8,9] which is abundant and valuable natural source of low-cost silica and which can be utilized for large-scale extraction is slate.

Slate is a metamorphic rock formed by the aggregation of tiny clay particles when stressed at high pressure for a long

Received: November 20, 2021
Accepted: January 31, 2022
Published: February 11, 2022

https://doi.org/10.1021/acsomega.1c06553
ACS Omega 2022, 7, 6113−6120

Table 1. Chemical Composition of Uncalcined, Calcined, and Acid Washed Slate Samples and Extracted Silica

	wt %								
	SiO_2	Al_2O_3	Fe_2O_3	CaO	MgO	K_2O	Na_2O	moisture	LOI
slate (raw)	63.9	17.1	5.9	3.9	2.3	3.1	3.1	0.1	0.6
slate (calcined and acid leached)	75.4	10.9	3.5	2.9	1.9	2.6	2.8		
extracted silica (after drying)	98.2	0.3	0.02	0.2	0.2	0.1	0.9	0.1	

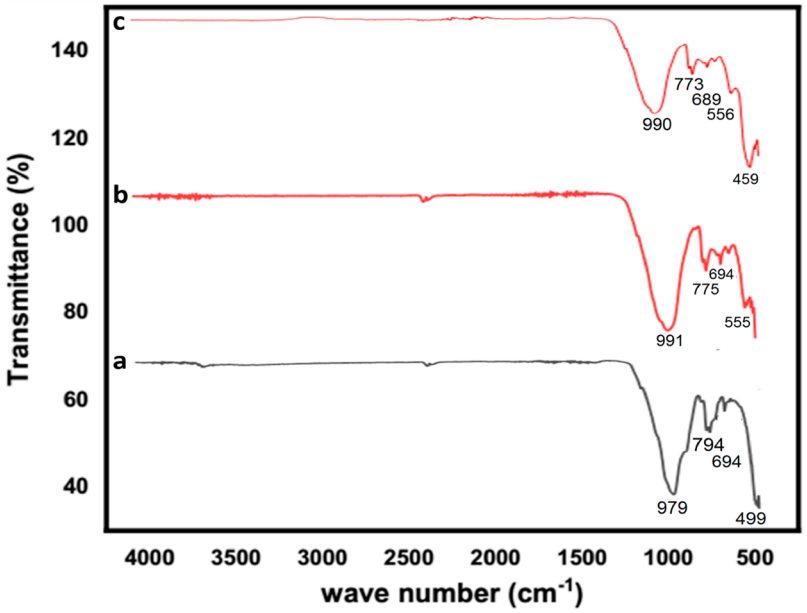

Figure 1. FT-IR spectra of (a) uncalcined slate sample, (b) calcined slate sample, and (c) extracted silica

time period. It is a mixture of silica and other insoluble minerals in a combined state. As reported in United States Geological Survey Bulletin No. 586, different slates of different regions have different chemical compositions, i.e., 54−69% silica (SiO_2), 10−25% alumina (Al_2O_3), 0.8−7.8% iron(III) oxide (Fe_2O_3), 0.1−5.1% calcium oxide (CaO), 1.5−6.4% magnesium oxide (MgO), 1.1−5.5% potassium oxide (K_2O), and 0.1−7.4% of sodium oxide (Na_2O).[10] The reported data indicated that these metamorphic rocks of slate are rich in silica. This silica can be extracted in amorphous form by performing several different unit operations including quarrying, crushing, and grinding followed by subsequent steps of calcination and hydrothermal treatment.

Different methods have been employed to extract silica from various raw materials by alkaline hydrothermal treatment. These raw materials include alkyl silicates, rice husk ash, coal fly ash, bagasse bottom ash, and clay. In 1968, Stober et al. prepared uniform spherical silica particles in alcoholic medium by hydrolysis of alkyl silicate and subsequent addition of ammonia.[11] In 2010, Zhang et al. obtained superfine silica nanoparticles from acid-treated rice husk ash.[12] The diameter of the silica ranged from 30 to 200 nm. In 2013, Liu et al. synthesized silica from acid-treated coal fly ash in the synthesis of mesoporous sieves for mercury removal by adsorption.[13] In 2016, Zulfiqar et al. utilized clay as a source material and synthesized silica nanoparticles.[3] In 2018, Bunmai et al. developed zeolite from silica (99.34% pure), which was obtained from cogon grass.[14] In 2021, Kamari and Ghorbani extracted silica from rice husk ash and studied its application in the production of magnetic mesoporous silica.[15] Most of the studies focused on synthesis of silica from fly and bottom ashes. This research is focused on the introduction of slate as a new and cheap raw material for the first time to obtain low cost, pure, and amorphous silica through hydrothermal treatment after calcination. In addition, the physical and chemical properties of slate are much better than fly and bottom ashes as slate is found in nature as a metamorphic rock whereas fly and bottom ashes can be obtained only after the combustion of carbonaceous materials. Furthermore, comparison the chemical composition of slate with fly and bottom ashes mainly shows silica. Because of these characteristic features of slate, it is used in the extraction of silica from natural resources.

RESULTS AND DISCUSSION

Characterization of Raw Material. The chemical composition of the slate sample determined by XRF analysis is provided in Table 1. The results show that the slate sample contains silica in a greater quantity, i.e., 63.9%, along with other major constituents, including Al_2O_3, Fe_2O_3, CaO, MgO, K_2O, and Na_2O. For maximum removal of other constituents, the ground slate was calcined at 900 °C for 1 h to decompose slate compounds followed by acid leaching to remove these free compounds along with other impurities. A significant change in the result of other major constituents was observed in calcined and acid-leached slate samples as shown in Table 1. The silica content increased to 75.4% due to the decrease of other constituents. An increase in silica content was found at 11.52%, while the alumina content decreased by 6.1% for the mass of calcined slate. The leaching of the calcined slate was carried out by using 1 M HCl solution at the sample to acid volume (gm: mL) ratio of 1:15. This ratio was based on

https://doi.org/10.1021/acsomega.1c06553
ACS Omega 2022, 7, 6113−6120

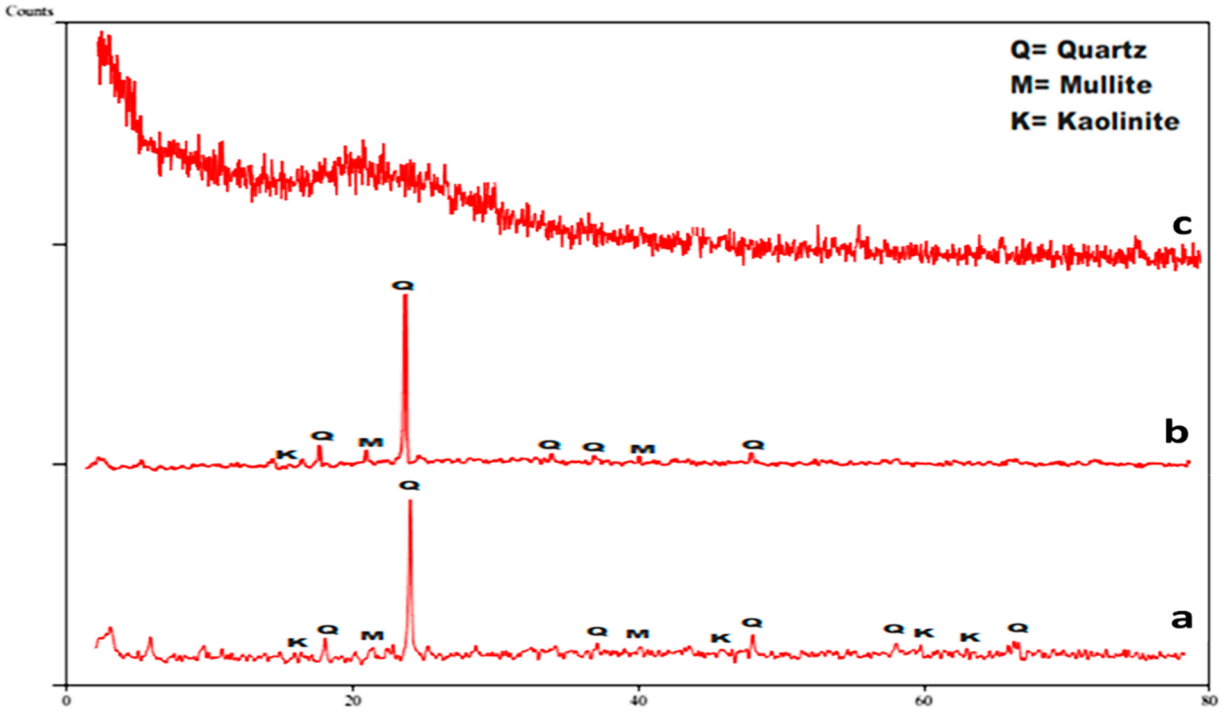

Figure 2. XRD pattern of uncalcined slate sample (a), calcined slate sample (b), and extracted silica (c).

stoichiometric calculations because the number of moles of alumina in 1 g of calcined slate is almost equal to the number of moles of HCl in 15 mL of 1 M concentration. Tantawy and Alomari[16] removed 75% of alumina from kaolin activated at 850 °C by an acid-leaching process, whereas Mark et al. recovered 50.27% of alumina by leaching of calcined Ibere clay, using 1 M HCl solution.[17] For this reason, about 59% of the total alumina has been leached while the rest remained recalcitrant which is evident from the XRF analysis provided in Table 1. In earlier research, the investigators analyzed 36 different samples of clay and reported a maximum of 66.8% SiO_2 and 21% Al_2O_3.[18]

The FT-IR spectra of slate samples before and after calcination (not acid leached) are shown in Figure 1. The spectra give a detailed explanation of the qualitative and quantitative features of the order and disorder in the bonding and structure before and after activation, depending upon the relative intensities of the various bonds including Si−O of SiO_4 and Al−O of AlO_4 in the range of 490−1000 cm^{-1}.[19] The band in the FT-IR spectrum of the uncalcined slate sample at 505 cm^{-1} is attributed to Si−O bond bending vibrations. In addition, relatively well-resolved bands appearing at 694 and 777 cm^{-1} are associated with the Al−O bending vibration. A broadband at 979 cm^{-1} may be assigned to the Si−O stretching vibration.[20] The change in structural features of the slate sample after calcination was recorded by collecting its FT-IR spectrum as shown in Figure 1b. The change of position and intensities of the characteristic peaks of slate and appearance of new peaks after the calcination indicate the high-temperature results in the decomposition of slate compounds. The results show that the peaks due to Si−O bond bending vibrations and Si−O stretching vibrations shifted to higher frequency, whereas the two bands due to the Al−O bond in the uncalcined slate sample change to triple bands after calcination. The shifting of the Si−O peaks from 977 to 991 cm^{-1} and from 505 to 522 cm^{-1} and transmutation of the two bands of the Al−O bond to triplet bands at 586, 694, and 781 cm^{-1} indicate the conversion of aluminum silicate compounds into the amorphous state of silica and alumina.[21]

Figure 2 shows the XRD patterns of the uncalcined and calcined slate samples before acid leaching. It can be observed that both patterns are characterized by the different numbers of quartz, mullite, and kaolinite peaks. In the slate sample after calcination, an amorphous phase can be seen in the range of 7 to 19° and 57 to 70°. In the uncalcined slate sample, various peaks due to kaolinite and quartz exist in these ranges, which have disappeared after calcination and replaced with an amorphous band indicating the transformation of the crystalline form of kaolinite and quartz to their amorphous form. Calcination at high temperature may lead to its dehydroxylation,[22] which increases the reactivity of alumina including other slate components, and can be easily extracted by using acid leaching process.[23,24] The XRF analysis provided in Table 1 can be used to support this argument as the percentage of alumina along with those of other major constituents were significantly decreased by acid leaching.

The surface morphologies of uncalcined and calcined slate (not acid leached) were studied by scanning electron microscopic, and their analysis is provided in Figure 3. The SEM micrograph as represented in Figure 4b shows the morphological transformations upon calcination. Figure 4a shows that uncalcined slate containing unevenly distributed different sized flakes. After activation, these flakes are found detached from each other and are dispersed oddly.

Condition Optimization for Maximum Silica Extraction. The maximum extraction of silica from calcined and acid leached slate sample mainly depends on the concentration of the alkaline solution. When the concentration is high, more amorphous silica reacts to form sodium silicate solution. The

https://doi.org/10.1021/acsomega.1c06553
ACS Omega 2022, 7, 6113−6120

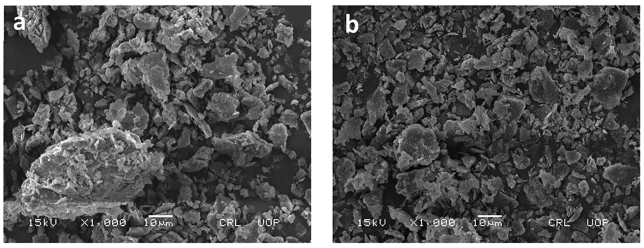

Figure 3. SEM images of (a) uncalcined slate sample and (b) calcined slate sample.

effect of the molar concentration of sodium hydroxide solution on the silica extraction is given in Figure 4a. The figure reveals that the silica extraction increases as the concentration of sodium hydroxide solution increases up to 1.5 M. Above this concentration, the amount of silica is observed to decrease; hence, 1.5 M concentration is the optimized concentration.

The effect of reaction time on the silica extraction is provided in Figure 4b. It is found that reaction time has a greater influence on the efficiency of silica extraction. As the reaction time increases from 20 to 60 min, an increase in the extraction of silica was observed. Above 60 min, silica extraction almost remained constant. It shows that the reaction of the entire amorphous silica completes with sodium hydroxide at 60 min and further that reaction time has no significant effect on the amount of extracted silica.

The effect of volume of alkaline solution of NaOH of 1.5 M compared to the fixed amount of the slate sample on silica extraction also plays an important role because as the volume of alkaline solution increases more silica molecules react with alkali. The result of the ratio of the mass of sample to volume of the alkaline solution is shown in Figure 4c which reveals that silica extraction increases as the volume of sodium hydroxide solution increase 20 times compared to the mass of calcined and acid leached slate sample. Further increase in volume has no better performance and the result was almost found constant which indicates that silica completes reaction with this volume of optimized alkali solution.

Effect of pH adjustment of the filtrate obtained after the hydrothermal reaction is given in Figure 4d which showed that the precipitation of silica started at a pH range of 5 to 12. Beyond this range, no silica appeared to precipitate. It may be due to greater solubility or redissolution of extracted silica in both strongly acidic and basic environments. Maximum extraction was observed when the pH of the filtrate was adjusted at 8.0.

The temperature effect on silica extraction was studied and is provided in Figure 4e. The results indicate that as the temperature increases the percent extraction of silica also increases. This is due to the inert and slight acidic nature of silica, which upon treatment with NaOH solution at high temperature gives better results.[25]

Analysis of Extracted Silica. The moisture content and purity of extracted silica under optimized conditions are provided in Table 1. The experimental results show that the maximum possible purity of extracted silica is approximately 98.2%. The result also shows close agreement with the XRF analysis of extracted silica as provided in Table 1 and Figure 5. Kalapathy et al.[26] and Velmurugan et al.[27] reported the maximum purity of silica obtained from rice husk ash and corn cob ash up to 60%, while Amin et al.[4] obtained 96% amorphous silica from bagasse ash by a hydrothermal reaction.

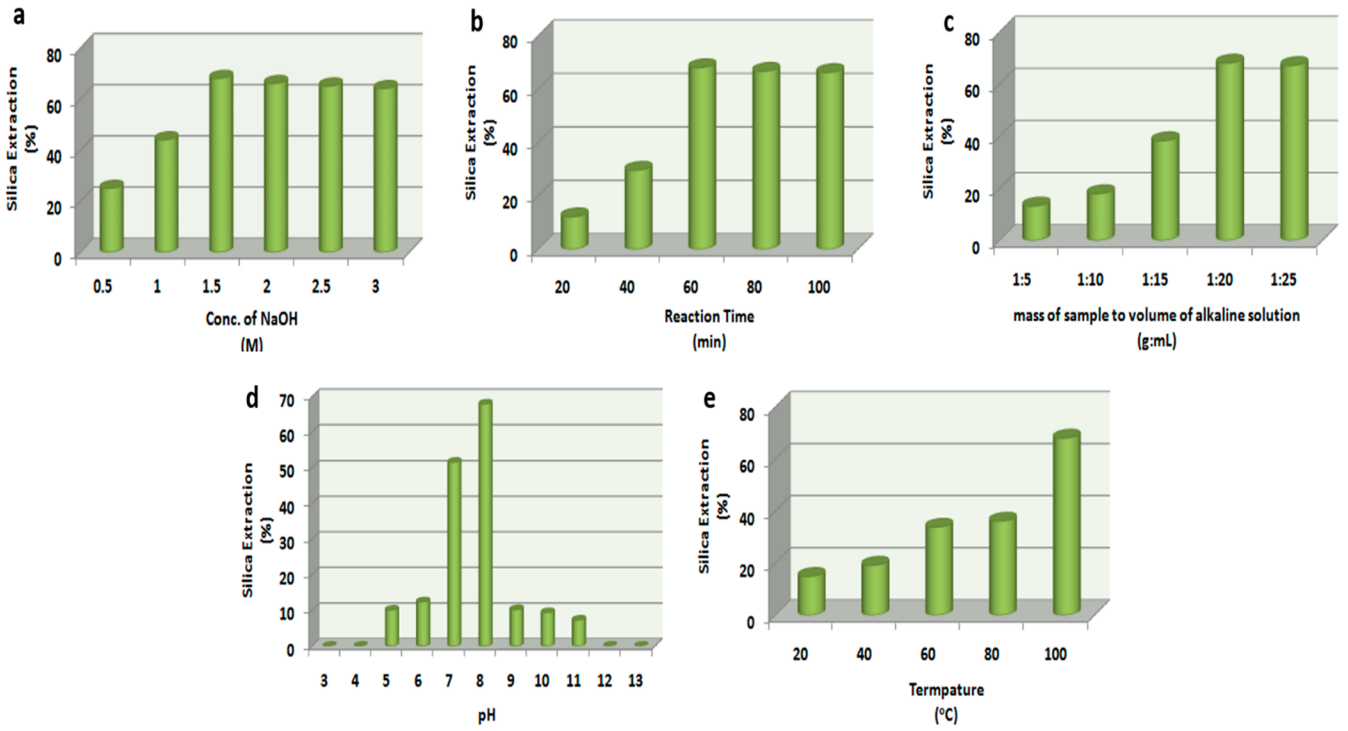

Figure 4. Condition optimization for maximum silica extraction: (a) effect of the molar concentration of NaOH solution (0.5−3 M), (b) effect of reaction time (20−100 min), (c) effect of the ratio of the mass of sample to volume of alkaline solution (1:5 to 1:25), (d) effect of pH (3−13), and (e) effect of temperature (20−100 °C).

https://doi.org/10.1021/acsomega.1c06553
ACS Omega 2022, 7, 6113−6120

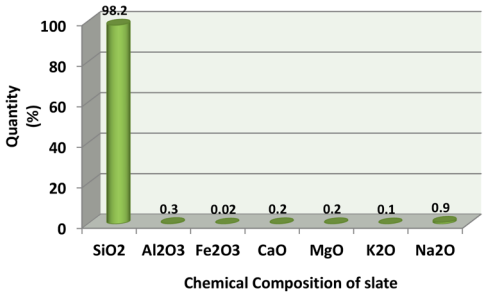

Figure 5. Chemical composition of extracted silica under optimized conditions.

Characterization of Extracted Silica. The chemical composition of the dried extracted silica was determined by using XRF analysis as provided in Table 1. The result shows that extracted silica is mainly composed of SiO_2, i.e., 98.2%, along with other constituents in trace amounts including Al_2O_3, Fe_2O_3, CaO, MgO, K_2O, and Na_2O. The presence of these elements in trace amounts may be due to the insufficient acid leaching of the calcined slate sample before silica extraction.

The FT-IR spectrum of the dried silica extracted under optimized conditions is provided in Figure 1c. The spectrum is characterized by all major peaks in the range 450−1000 cm^{-1}. Sharp peaks at 990 and 556 cm^{-1} are assigned to the asymmetric stretching vibration of the Si−O−Si,[27,28] while peaks at 680−780 cm^{-1} are correlated to symmetric vibration of the Si−O−Si bond. On the other hand, the peaks that appeared in the range of 420−460 cm^{-1} are due to the bending vibration of O−Si−O bonds.[29]

XRD patterns of silica obtained from the calcined and acid-leached slate sample is represented in Figure 2c. The pattern confirms that the nature of the extracted silica is characteristically amorphous. The diffraction peaks at 20−24 2-θ also prove the formation of amorphous silica. It may be due to the disordered of cristobalite.[30] The XRD pattern obtained in the current study shows close agreement with XRD patterns obtained in the previous investigations.[31,32]

SEM micrographs of the amorphous silica with different magnifications extracted under optimized conditions are provided in Figure 6. The figures reveal that silica mostly comprises the very small size of irregularly arranged particles and shows a tendency toward aggregation to form comparatively larger particles. The SEM images show that the surface of the extracted silica is characterized by several pores; thus, it can be used as a novel adsorbent for the removal of different toxic materials like heavy metals, dyes, etc. by adsorption.

Advantages of Silica. The experimental results showed the extraction of an appreciable amount of amorphous silica from naturally abundant sources, indicating the great success of the current research over the previous studies. Industrially, the maximum amount of amorphous silica can be obtained from calcined and acid-leached slate by using the optimized conditions. The process involves calcination, acid leaching, and extraction, which may increase the cost of silica, but due to the very low price of slate and widespread industrial applications including water desalination by reverse osmosis[33] and the synthesis of silica−graphene-based nanocomposite,[34] silica nanoparticles,[35] and ligand anchor based adsorbent,[36] etc. make slate a suitable option for silica extraction. As a technical quality of the current study, this method can be employed to other natural resources to obtain silica.

CONCLUSIONS

In the current study, the hydrothermal process was studied to extract the maximum amount of pure amorphous silica, and the following conclusions were made:

(i) Calcination of ground slate followed by acid leaching significantly reduces the alumina and other major constituents and results in increased silica content.
(ii) The calcined and acid-leached slate sample can be used as an excellent source of amorphous silica, which can be obtained by hydrothermal extraction.
(iii) The maximum amount of pure amorphous silica was successfully obtained when the calcined and acid-leached sample was boiled for 60 min in 1.5 M sodium hydroxide solution at a 1:20 (g:mL) ratio.
(iv) The amorphous nature of the extracted silica was confirmed by XRD and SEM analyses.
(v) The FT-IR spectrum of silica reveals the presence of only Si−O−Si bonds. The elemental composition showed that the extracted silica is 98.2% pure.

MATERIALS AND METHODS

Materials. A natural and rich source of silica, i.e., slate, was collected from the Chashmai mines in the District Nowshera, Khyber Pakhtunkhwa, Pakistan. The selected slate sample was

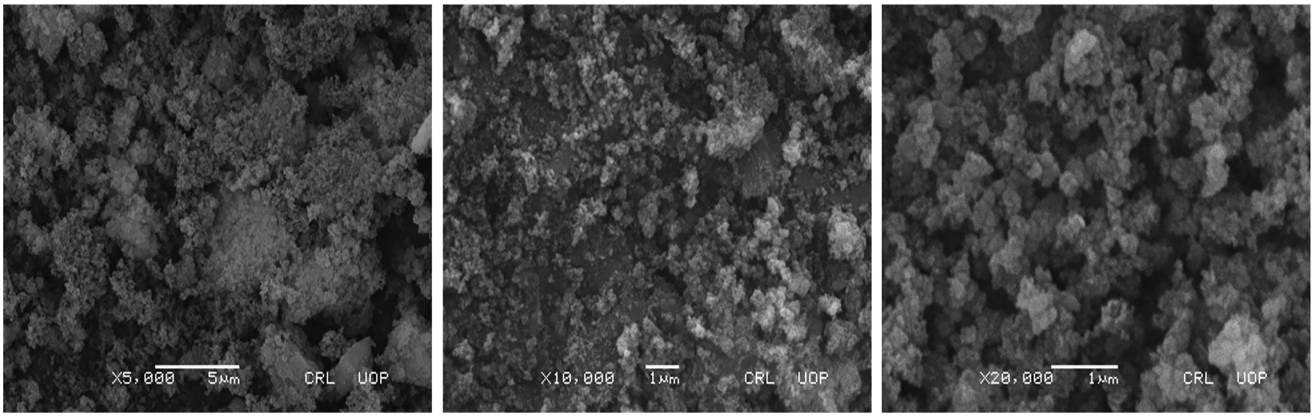

Figure 6. SEM images of extracted silica with different magnifications.

https://doi.org/10.1021/acsomega.1c06553
ACS Omega 2022, 7, 6113−6120

converted into a fine powder using a grinder to increase the surface area to maximize silica extraction. The powdered sample was meshed through a 250 μm sieve. Pellets of analytical grade sodium hydroxide (NaOH) were procured from Sigma-Aldrich Co, St. Louis, MO, while analytical grade hydrochloric acid (37%) was purchased from Merck. Distilled water was used for washing and solution preparation.

Calcination of Powdered Slate. Powdered samples of slate were calcined at 900 °C in a muffle furnace working up to 1100 °C. The incremental heating rate was maintained at 15 °C/min, and the time of residence was kept at 1 h. Calcined samples were then allowed to cool to room temperature in a desiccator. After cooling, the calcined sample was powdered in a grinding machine until 100% of the mass had passed a 250 μm mesh.

Acid Leaching of Calcined Powder Slate. Acid leaching of ground calcined slate was carried out to remove impurities for obtaining pure silica. A mass of 10 g of powdered calcined slate sample was added to 150 mL of 1 M hydrochloric acid solution and boiled for 1 h with constant stirring. The mixture was filtered through Whatman filter paper 41 (pore size 20 μm) to separate a silica-rich slate sample. The residue was thoroughly washed with hot distilled water (60 °C) until the pH was 7 and then dried in an oven until a constant weight was obtained. This dried sample was utilized for alkaline hydrothermal extraction of silica.

Silica Extraction. For extraction of pure silica, 1 g of acid leached calcined slate sample was dispersed in 20 mL of 1.5 M sodium hydroxide solution according to the exact stoichiometric ratio calculated from the following balanced chemical equation:

$$Na_2SiO_{3(aq)} + 2HCl_{(aq)} \rightarrow SiO_{2(s)} + 2NaCl_{(aq)} + H_2O$$

The dispersion was boiled in a round-bottom flask fitted with a reflux condenser by indirect heating in a container filled with lubricating oil (bp > 200 °C) on a hot plate with constant stirring for 60 min. Time counting was noted after the boiling of dispersion. The reflux condenser was sealed at the top to prevent water loss from the dispersion by evaporation, which may affect the concentration of NaOH solution. The mixture was filtered using Whatman filter paper 41, and the residue was washed with hot distilled water for maximum removal of dissolved silica. The resultant filtrate was cooled at room temperature followed by dropwise addition of 9.5 mL of 1 M HCl solution under constant stirring. Finally, precipitated silica appeared. As a result of the addition of acid, the pH of the solution dropped to 8. The utilization of a fixed volume of 1 M HCl solution was computed by stoichiometric calculation using the following chemical equation:

$$Na_2SiO_{3(aq)} + 2HCl_{(aq)} \rightarrow SiO_{2(s)} + 2NaCl_{(aq)} + H_2O$$

The precipitated silica was allowed to stand for 24 h at room temperature in the mother liquor followed by centrifugation to obtain a white powder of pure silica. The obtained silica was repeatedly washed with hot distilled water to remove residual impurities and dried at 105 °C until a constant weight was obtained. The produced NaCl was removed from the mother liquor before discarding by crystallization to minimize the potential effluents.

Condition Optimization for Maximum Extraction Silica. Different conditions including concentration of sodium hydroxide solution, reaction time, the ratio of the mass of sample to volume of alkaline solution, filtrate pH, and the temperature of dispersion were optimized step-by-step for maximum extraction of silica in the following pattern:

(i) The different concentrations of sodium hydroxide solution used in the experiments were 0.5, 1, 1.5, 2, 2.5, and 3 M, while the reaction time, ratio of the mass of sample to volume of alkaline solution, filtrate pH, and temperature of dispersion were kept constant at 20 min, 1:10, 7, and 20 °C, respectively. This concentration is in accordance with the available literature. Liou and Yang[2] reported 1.5 M, Zulfiqar et al.[3] used a 2 M solution of NaOH while Amin et al.[21] utilized a 1.5 N NaOH solution for silica extraction.

(ii) The effect of the reaction time on silica extraction was studied between 20 and 100 min using an optimized concentration (1.5 M) of sodium hydroxide solution, 1:10 ratio of the mass of sample to volume of alkaline solution, maintaining pH = 7 of the filtrate and 20 °C temperature of the dispersion.

(iii) The ratio of the mass of sample to volume of alkaline solution was maintained at 1:5, 1:10,1:15, 1:20, and 1:25. Other test conditions including 1.5 M sodium hydroxide solution (optimized), 60 min of reaction time (optimized), pH = 7 of the filtrate and 20 °C as temperature of dispersion were used.

(iv) The pH of the filtrate was adjusted at a value between 3 and 12 for maximum silica extraction. In this step, three optimized conditions including concentration of sodium hydroxide solution, reaction time, and ratio of the mass of sample to volume of alkaline solution, i.e., 1:20, were employed at a constant temperature of 20 °C.

(v) The effect of heating was studied between 20 and 100 °C at an optimized concentration of sodium hydroxide solution, reaction time, the ratio of the mass of sample to volume of alkaline solution, and filtrate pH = 8 (optimized).

For each optimization step, the quantity of extracted silica was calculated by eq 1:

$$\text{quantity of silica (\%)} = \frac{\text{mass of extracted silica}}{\text{mass of acid washed calcine slate sample}} \times 100 \quad (1)$$

Analysis of Extracted Silica. The extracted silica was analyzed for moisture content and purity. The moisture content was calculated according to a method reported by Okoronkwo et al.[37] About 1 g (W_1) of extracted silica was heated in the air in an oven at 130 °C in an aluminum moisture pan for 1 h. The silica sample was then cooled to room temperature in a desiccator and again weighed (W_2) to find the weight loss in terms of percentage by eq 2:

$$\text{moisture contents of silica (\%)} = \frac{W_1 - W_2}{W_1} \times 100 \quad (2)$$

The purity of the dried extracted silica was estimated according to the method reported by Amin, Noor-ul, et al.[4] The extracted silica was mixed with 48% of hydrofluoric acid (HF) at a ratio of 2:1 (g: mL) in a platinum crucible, and the weight (W_1) was noted. The mixture was then heated in a muffle furnace until constant weight followed by cooling in a desiccator and again weighed (W_2). The purity was determined from eq 3:

https://doi.org/10.1021/acsomega.1c06553
ACS Omega 2022, 7, 6113−6120

$$\text{Purity of silica}(\%) = \frac{W1 - W2}{W1} \times 100 \quad (3)$$

Characterization of Raw Material and Extracted Silica. The raw material and the extracted silica samples were studied through different analytical techniques. The elemental composition was analyzed using a Cubic XRF spectrometer (Model: PW2300, Netherland, Askari Cement Limited, Nizampur Nowshehra). The surface morphologies of both raw material and extracted silica were studied by using a scanning electron microscope (JEOL-JSM-5910; Japan, CRL University of Peshawar). Powder X-ray diffraction (XRD) patterns were obtained at the 2-θ angle (10−70°) using an X-ray diffractometer (JDX-9C, JEOL, Japan, University of Peshawar) at room temperature with CuKα radiation and a nickel filter. Fourier transform infrared spectroscopic studies were performed using an FT-IR spectrophotometer (PerkinElmer Spectrum, Version 10.4.00, Bacha Khan University, Charsadda) in the wavenumber range of 4000−400 cm^{-1}.

AUTHOR INFORMATION

Corresponding Authors

Abid Zaman − *Department of Physics, Riphah International University, Islamabad 44000, Pakistan;* orcid.org/0000-0001-9527-479X; Email: zaman.abid87@gmail.com

Asad Ali − *Department of Physics, Government Postgraduate College, Nowshera 24100 KPK, Pakistan; Department of Physics, Riphah International University, Islamabad 44000, Pakistan*; Email: kasadiiui@gmail.com

Authors

Usman Ghani − *Department of Chemistry, Government Postgraduate College, Nowshera 24100 KPK, Pakistan*

Shah Hussain − *Department of Chemistry, Government Postgraduate College, Nowshera 24100 KPK, Pakistan*

Vineet Tirth − *Mechanical Engineering Department, College of Engineering, King Khalid University, Abha 61421 Asir, Kingdom of Saudi Arabia; Research Center for Advanced Materials Science (RCAMS), King Khalid University Guraiger, Abha 61413 Asir, Kingdom of Saudi Arabia*

Ali Algahtani − *Mechanical Engineering Department, College of Engineering, King Khalid University, Abha 61421 Asir, Kingdom of Saudi Arabia; Research Center for Advanced Materials Science (RCAMS), King Khalid University Guraiger, Abha 61413 Asir, Kingdom of Saudi Arabia*

Muhammad Mushtaq − *Faculty of Materials Science, Beijing University of Technology, Beijing 100124, China*

Khaled Althubeiti − *Department of Chemistry, College of Science, Taif University, Taif 21944, Saudi Arabia*

Mohammed Aljohani − *Department of Chemistry, College of Science, Taif University, Taif 21944, Saudi Arabia*

Complete contact information is available at: https://pubs.acs.org/10.1021/acsomega.1c06553

Author Contributions

This work was carried out in collaboration among all authors. U.G. and S.H. prepared samples and wrote the original draft of the manuscript. A.Z., V.T., and A.A. did the final writing review, corrections, and editing. A.A. and M.M. prepared the content analysis and software and graphical arrangements. M.A. and K.A. helped with the formal analysis and validation and provided funding acquisition. All authors read and approved the final manuscript.

Notes

The authors declare no competing financial interest.

ACKNOWLEDGMENTS

Taif University Researchers Supporting Project No. (TURSP-2020/241), Taif University, Taif, Saudi Arabia. The authors V.T. and A.A. gratefully acknowledge the Deanship of Scientific Research, King Khalid University (KKU), Abha-Asir, Kingdom of Saudi Arabia, for funding this research work under the Grant No. R.G.P.2/89/41.

REFERENCES

(1) An, D.; Guo, Y.; Zhu, Y.; Wang, Z. A green route to preparation of silica powders with rice husk ash and waste gas. *Chem. Eng. J.* **2010**, *162*, 509−514.

(2) Liou, T.-H.; Yang, C.-C. Synthesis and surface characteristics of nanosilica produced from alkali-extracted rice husk ash. *Mater. Sci. Eng., B* **2011**, *176*, 521−529.

(3) Zulfiqar, U.; Subhani, T.; Husain, S. W. Synthesis and characterization of silica nanoparticles from clay. *J. Asian. Ceram. Soc.* **2016**, *4*, 91−96.

(4) Amin, N.-U.; Khattak, S.; Noor, S.; Ferroze, I. Synthesis and characterization of silica from bottom ash of sugar industry. *J. Cleaner Prod.* **2016**, *117*, 207−211.

(5) Schlomach, J.; Kind, M. Investigations on the semi-batch precipitation of silica. *J. Colloid Interface Sci.* **2004**, *277*, 316−326.

(6) Witoon, T.; Chareonpanich, M.; Limtrakul, J. Synthesis of bimodal porous silica from rice husk ash via sol−gel process using chitosan as template. *Mater. Lett.* **2008**, *62*, 1476−1479.

(7) Zaky, R. R.; Hessien, M. M.; El-Midany, A. A.; Khedr, M. H.; Abdel-Aal, E. A.; El-Barawy, K. A. Preparation of silica nanoparticles from semi-burned rice straw ash. *Powder Technol.* **2008**, *185*, 31−35.

(8) Zawrah, M.; El-Kheshen, A. A.; Abdelaal, H. Facile and Economic Synthesis of Silica Nanoparticles. *J. Ovonic Res.* **2009**, *5*, 129−133.

(9) Choucair, M.; Thordarson, P.; Stride, J. A. Gram-scale production of graphene based on solvothermal synthesis and sonication. *Nat. Nanotechnol.* **2009**, *4*, 30−33.

(10) Kessler, D. W.; Sligh, W. H. Physical properties and weathering characteristics of slate. *Bur. Stand. J. Res.* **1932**, *9*, 377−384.

(11) Stöber, W.; Fink, A.; Bohn, E. Controlled growth of monodisperse silica spheres in the micron size range. *J. Colloid Interface Sci.* **1968**, *26*, 62−69.

(12) Zhang, H.; Zhao, X.; Ding, X.; Lei, H.; Chen, X.; An, D.; Li, Y.; Wang, Z. A study on the consecutive preparation of d-xylose and pure superfine silica from rice husk. *Bioresour. Technol.* **2010**, *101*, 1263−1267.

(13) Liu, M.; Hou, L.-A.; Xi, B.; Zhao, Y.; Xia, X. Synthesis, characterization, and mercury adsorption properties of hybrid mesoporous aluminosilicate sieve prepared with fly ash. *Appl. Surf. Sci.* **2013**, *273*, 706−716.

(14) Bunmai, K.; Osakoo, N.; Deekamwong, K.; Rongchapo, W.; Keawkumay, C.; Chanlek, N. Prayoonpokarach S, and Wittayakun J, Extraction of silica from cogon grass and utilization for synthesis of zeolite NaY by conventional and microwave-assisted hydrothermal methods. *J. Taiwan Inst. Chem. Eng.* **2018**, *83*, 152−158.

(15) Kamari, S.; Ghorbani, F. Extraction of highly pure silica from rice husk as an agricultural by-product and its application in the production of magnetic mesoporous silica MCM−41. *Biomass Convers. Biorefin.* **2021**, *11*, 3001−3009.

(16) Tantawy, M.; Alomari, A. Extraction of Alumina from Nawan Kaolin by Acid Leaching. *Orient. J. Chem.* **2019**, *35*, 1013−1021.

(17) Mark, U.; Anyakwo, C. N.; Onyemaobi, O. O.; Nwobodo, C. S. Effect of calcination condition on thermal activation of Ibere clay and dissolution of alumina. *Int. J. Nonferrous Metall.* **2019**, *8*, 9−24.

(18) Ufer, K.; Stanjek, H.; Roth, G.; Dohrmann, R.; Kleeberg, R.; Kaufhold, S. Quantitative phase analysis of bentonites by the rietveld method. *Clays Clay Miner.* **2008**, *56*, 272−282.

https://doi.org/10.1021/acsomega.1c06553
ACS Omega 2022, 7, 6113−6120

(19) Hajimohammadi, A.; Provis, J. L.; van Deventer, J. S. J. One-Part Geopolymer Mixes from Geothermal Silica and Sodium Aluminate. *Ind. Eng. Chem. Res.* **2008**, *47*, 9396−9405.
(20) Nath, D. C. D.; Bandyopadhyay, S.; Gupta, S.; Yu, A.; Blackburn, D.; White, C. Surface-coated fly ash used as filler in biodegradable poly(vinyl alcohol) composite films: Part 1—The modification process. *Appl. Surf. Sci.* **2010**, *256*, 2759−2763.
(21) Noor-ul-Amin; Faisal, M.; Muhammad, K.; gul, S. Synthesis and characterization of geopolymer from bagasse bottom ash, waste of sugar industries and naturally available china clay. *J. Cleaner Prod.* **2016**, *129*, 491−495.
(22) Żymankowska-Kumon, S.; Holtzer, M.; Olejnik, E.; Bobrowski, A. Influence of the Changes of the Structure of Foundry Bentonites on Their Binding Properties. *Mater. Sci.* **2012**, *18*, 57−61.
(23) Ohale, P. E.; Uzoh, C. F.; Onukwuli, O. D. Optimal factor evaluation for the dissolution of alumina from Azaraegbelu clay in acid solution using RSM and ANN comparative analysis. *S. Afr. J. Chem. Eng.* **2017**, *24*, 43−54.
(24) Megwai, G. Kinetics of Alumina Leaching of Calcined Clay Using Acids (Chloric, nitric and sulphuric acids). B.S. Thesis, 2009.
(25) Aphane, M. E.; Doucet, F. J.; Kruger, R. A.; Petrik, L.; van der Merwe, E. M. Preparation of Sodium Silicate Solutions and Silica Nanoparticles from South African Coal Fly Ash. *Waste Biomass Valorization.* **2019**, *11*, 4403−4417.
(26) Kalapathy, U.; Proctor, A.; Shultz, J. An improved method for production of silica from rice hull ash. *Bioresour. Technol.* **2002**, *85*, 285−289.
(27) Velmurugan, P.; Shim, J.; Lee, K.-J.; Cho, M.; Lim, S.-S.; Seo, S.-K.; Cho, K.-M.; Bang, K.-S.; Oh, B.-T. Extraction, characterization, and catalytic potential of amorphous silica from corn cobs by sol-gel method. *J. Ind. Eng. Chem.* **2015**, *29*, 298−303.
(28) Amin, N-u. A multi-directional utilization of different ashes. *RCS Adv.* **2014**, *4*, 62769−62788.
(29) Setyawan, N.; Hoerudin; Wulanawati, A. Simple extraction of silica nanoparticles from rice husk using technical grade solvent: effect of volume and concentration. *IOP Conference Series: Earth and Environmental Science.* **2019**, *309*, 012032.
(30) Damby, D. E.; Llewellin, E. W.; Horwell, C. J.; Williamson, B. J.; Najorka, J.; Cressey, G.; Carpenter, M. The α-β phase transition in volcanic cristobalite. *J. Appl. Crystallogr.* **2014**, *47*, 1205−1215.
(31) Musić, S.; Filipović-Vinceković, N.; Sekovanić, L. Precipitation of amorphous SiO2 particles and their properties. *Braz. J. Chem. Eng.* **2011**, *28*, 89−94.
(32) Nallathambi, G.; Ramachandran, T.; Venkatachalam, R.; Palanivelu, R. Effect of Silica Nanoparticles and BTCA on Physical Properties of Cotton Fabrics. *Mater. Res.* **2011**, *14*, 552−559.
(33) Park, Y.-M.; Yeon, K.-M.; Park, C-h. Silica treatment technologies in reverse osmosis for industrial desalination: A review. *Environ. Eng. Res.* **2020**, *25*, 819−829.
(34) Ma, M.; Li, H.; Xiong, Y.; Dong, F. Rational design, synthesis, and application of silica/graphene-based nanocomposite: A review. *Mater. Des.* **2021**, *198*, 109367.
(35) Porrang, S.; Rahemi, N.; Davaran, S.; Mahdavi, M.; Hassanzadeh, B. Preparation and in-vitro evaluation of mesoporous biogenic silica nanoparticles obtained from rice and wheat husk as a biocompatible carrier for anti-cancer drug delivery. *Eur. J. Pharm. Sci.* **2021**, *163*, 105866.
(36) Awual, M. R.; Hasan, M. M.; Iqbal, J.; Islam, A.; Islam, M. A.; Asiri, A. M.; Rahman, M. M. Naked-eye lead(II) capturing from contaminated water using innovative large-pore facial composite materials. *Microchem. J.* **2020**, *154*, 104585.
(37) Okoronkwo, E. A.; Imoisili, P.; Olusunle, S. Extraction and characterization of amorphous silica from corn cob ash by sol-gel metho[d]. *Chem. Mater. Res.* **2013**, *3*, 68−72.

https://doi.org/10.1021/acsomega.1c06553
ACS Omega 2022, 7, 6113−6120